

Measurement report: Oxidation potential of water-soluble aerosol components in the southern and northern of Beijing

Wei Yuan¹, Ru-Jin Huang¹, Chao Luo², Lu Yang¹, Wenjuan Cao¹, Jie Guo¹, Huinan Yang²

¹State Key Laboratory of Loess and Quaternary Geology, Center for Excellence in Quaternary Science and Global Change, Institute of Earth Environment, Chinese Academy of Sciences, Xi'an 710061, China.

²School of Energy and Power Engineering, University of Shanghai for Science and Technology, Shanghai 200093, China

Correspondence: Ru-Jin Huang (rujin.huang@ieecas.cn) and Huinan Yang (yanghuinan@usst.edu.cn)

Abstract

Water-soluble components have significant contribution to the oxidative potential (OP) of atmospheric fine particles (PM_{2.5}), while our understanding of water-soluble PM_{2.5} OP and its sources, as well as its relationship with water-soluble components, ~~their relationship~~ is still limited. In this study, the water-soluble OP levels in wintertime PM_{2.5} in the south and north of Beijing, representing the difference in sources, were measured with dithiothreitol (DTT) assay. The volume normalized DTT (DTT_v) in the north ($3.5 \pm 1.2 \text{ nmol min}^{-1} \text{ m}^{-3}$) was comparable to that in the south ($3.9 \pm 0.9 \text{ nmol min}^{-1} \text{ m}^{-3}$), while the mass normalized DTT (DTT_m) in the north ($65.3 \pm 27.6 \text{ pmol min}^{-1} \mu\text{g}^{-3}$) was almost twice that in the south ($36.1 \pm 14.5 \text{ pmol min}^{-1} \mu\text{g}^{-3}$). In both the south and north of Beijing, DTT_v was better correlated with soluble elements instead of total elements. In the north, soluble elements (mainly Mn, Co, Ni, Zn, As, Cd and Pb) and water-soluble organic compounds, especially light-absorbing compounds (also known as brown carbon),

29 had positive correlations with DTT_v. However, in the south, the DTT_v was mainly
30 related to soluble As, Fe and Pb. The sources of DTT_v were further resolved using the
31 positive matrix factorization (PMF) model. Traffic-related emissions (39.1%) and
32 biomass burning (25.2%) were the main sources of DTT_v in the south, and traffic-
33 related emissions (> 50%) contributed the most of DTT_v in the north. Our results
34 indicate that vehicle emission was the important contributor to OP in Beijing ambient
35 PM_{2.5} and suggest that more study is needed to understand the intrinsic relationship
36 between OP and light absorbing organic compounds.

37

38 **1 Introduction**

39 Atmospheric fine particulate matter (PM_{2.5}) pollution is one of the major global
40 environmental issues, affecting air quality, climate and human health (Huang et al.,
41 2014; Burnett et al., 2018; An et al., 2019; Zheng et al., 2020). The exposure to PM_{2.5}
42 was estimated to be responsible for 8.9 million deaths worldwide in 2015, of which
43 28% occurred in China (Burnett et al., 2018). Numerous studies have shown that
44 oxidative stress is one of the main mechanisms underlying the adverse effects of
45 PM_{2.5} on human health (Chowdhury et al., 2019; Lelieveld et al., 2021; Yu et al.,
46 2022b). When entering the human body, PM_{2.5} can induce the production of excessive
47 reactive oxygen species (ROS) (e.g., H₂O₂, ·OH and ·O₂⁻), leading to cellular redox
48 imbalance and generating oxidative stress effects. The ability of PM_{2.5} to cause
49 oxidative stress is defined as oxidative potential (OP).

50 The methods to determine the OP of PM_{2.5} include cellular and acellular assays,
51 and acellular methods are more widely used than cellular methods (Charrier and
52 Anastasio, 2012; Xiong et al., 2017; Calas et al., 2018; Bates et al., 2019; Wang et al.,
53 2020b; Campbell et al., 2021; Oh et al., 2023). Among acellular methods, the
54 dithiothreitol (DTT) assay is extensively applied to determine the OP of ambient
55 particles (Charrier and Anastasio, 2012; Xiong et al., 2017; Liu et al., 2018; Wang et
56 al., 2020b; Puthussery et al., 2022; Wu et al., 2022a). DTT is a surrogate of cellular
57 reductants, and the consumption rate of DTT was used to assess the OP of PM_{2.5}.

58 Previous studies have shown that organic matters (e.g., water-soluble organic species
59 and PAHs) and some transition metals (e.g., Mn and Cu) are the important
60 contributors to DTT consumption of PM_{2.5} (Charrier and Anastasio, 2012; Verma et
61 al., 2015; Bates et al., 2019; Wu et al., 2022a; Wu et al., 2022b). For example,
62 Charrier and Anastasio (2012) measured the OP of PM_{2.5} in San Joaquin Valley,
63 California and reported that about 80% of DTT consumption was contributed by
64 transition metals. Verma et al. (2015) measured the OP of water-soluble PM_{2.5} in the
65 southeastern United States and reported that about 60% of DTT activity was
66 contributed by water-soluble organics. The mixtures of metals and organics may
67 produce synergistic or antagonistic effects, such as ·O₂⁻ produced from oxidation of
68 DTT by quinones is more efficiently transformed to ·OH in the presence of Fe, while
69 the DTT consumption and ·OH generation of quinones are reduced in the presence of
70 Cu (Xiong et al., 2017; Yu et al., 2018; Bates et al., 2019).

71 A number of studies have investigated the OP of water-soluble components in
72 PM_{2.5}, which show that the average water-soluble OP values in urban areas ranged
73 from 0.1 to 10 nmol min⁻¹ m⁻³ (Fang et al., 2016; Liu et al., 2018; Chen et al., 2019;
74 Wu et al., 2022a; Yu et al., 2022a; Xing et al., 2023). Due to the complexity in
75 chemical composition and sources of PM_{2.5} that determine the OP levels, the sources
76 of OP are also diverse (Verma et al., 2015; Bates et al., 2019; Tuet et al., 2019; Yu et
77 al., 2019; Cao et al., 2021). Several studies have investigated the emission sources and
78 ambient samples to identify the sources of OP (Tuet et al., 2019; Yu et al., 2019; Wang
79 et al., 2020b; Cao et al., 2021), which include both primary and secondary sources.
80 For example, Cao et al. (2021) measured the water-soluble OP of PM_{2.5} samples from
81 six biomass and five coal burning emissions in China, with average values of 4.5-7.4
82 and 0.5-2.1 pmol min⁻¹ μg⁻¹, respectively. Tong et al. (2018) investigated the OP of
83 secondary organic aerosols (SOA) from oxidation of naphthalene, isoprene and β-
84 pinene with ·OH or O₃, which were 104.4 ± 7.6, 48.3 ± 7.9 and 36.4 ± 3.1 pmol min⁻¹
85 μg⁻¹, respectively. Verma et al. (2014) identified the source of water-soluble OP of
86 PM_{2.5} in Atlanta, United States from June 2012 to September 2013 with positive

87 matrix factorization (PMF) and chemical mass balance (CMB) methods, of which
88 biomass burning was the largest contributor. Wang et al. (2020b) quantified the
89 sources of water-soluble OP of PM_{2.5} in Xi'an, China in 2017 using PMF and multiple
90 linear regression (MLR) methods, with significant contributions from secondary
91 sulfates, vehicle emissions and coal combustion. Despite these efforts, comparative
92 studies on the differences in pollution levels and sources of PM_{2.5} OP in different
93 districts are still limited.

94 In this study, the DTT activity of water-soluble matter in PM_{2.5} samples collected
95 simultaneously in the southern and northern of Beijing in January 2018 were
96 measured. The concentration and light absorption of water-soluble organic carbon
97 (WSOC), as well as the concentrations of 14 trace elements and 7 light-absorbing
98 nitroaromatic compounds (NACs) were quantified. The sources of DTT activity were
99 then identified with PMF model. The results acquired in this study provide a
100 ~~comprehensive~~ comparison of PM_{2.5} OP in different districts of Beijing and its
101 connection with organic compounds, trace elements and sources, which could be
102 helpful for further study of the regional differences in the effects of PM_{2.5} on human
103 health.

104

105 **2 Materials and methods**

106 **2.1 Sampling**

107 Ambient 24 h integrated PM_{2.5} filter samples were collected from January 1 to 31,
108 2018 simultaneously in the south (the Dingfuzhuang village (DFZ), Daxing district;
109 39.61°N, 116.28°E) and north (the National Center for Nanoscience and Technology
110 (NCNT), Haidian district; 39.99°N, 116.32°E) of Beijing (Figure S1). The distance
111 between the two sampling sites is about 42 km. The south site is surrounded by
112 agricultural, industrial, and transportation areas, and the north site is surrounded by
113 residential, transportation and commercial areas. PM_{2.5} samples were collected on pre-
114 baked (780 °C, 3 h) quartz-fiber filters (20.3 × 25.4 cm; Whatman, QM-A, Clifton, NJ,
115 USA) using high-volume PM_{2.5} samplers (1.13 m⁻³ min⁻¹; Tisch, Cleveland, OH, USA)

116 which were placed on the roof of buildings at heights of about 5 m (south) and 20 m
117 (north) above the ground. [31 samples were collected at each site.](#) After collection, the
118 samples were wrapped in baked aluminum foils and stored in a freezer ($-20\text{ }^{\circ}\text{C}$) until
119 further analysis.

120 **2.2 Chemical analysis**

121 The mass of $\text{PM}_{2.5}$ on the filter was measured by a digital microbalance with a
122 precision of 0.1 mg (LA130S-F, Sartorius, Germany) after 24-h equilibration at a
123 constant temperature ($20\text{-}23\text{ }^{\circ}\text{C}$) and humidity (35-45%) chamber. Each filter was
124 weighted at least two times, and the deviations for blank and sampled filters among
125 the repetitions were less than 5 and 10 μg , respectively. The $\text{PM}_{2.5}$ mass concentration
126 was calculated by dividing the weight difference before and after sampling by the
127 volume of sampled air.

128 For WSOC analysis, one punch (1.5 cm^2 for concentration analysis and 0.526
129 cm^2 for light absorption measurement) of filter was taken from each sample and
130 extracted ultrasonically with ultrapure water ($> 18.2\text{ M}\Omega\text{ cm}$) for 30 min. After, the
131 extracts were filtered with a $0.45\text{ }\mu\text{m}$ PVDF pore syring filter to remove insoluble
132 substances. Finally, the concentration of WSOC was measured with a total organic
133 carbon-total nitrogen analyzer (TOC-L, Shimadzu, Japan; (Ho et al., 2015)) and the
134 light absorption of WSOC was measured by an UV-Vis spectrophotometer ([300-700](#)
135 [nm; Ocean Optics, USA](#)) equipped with a liquid waveguide capillary cell (LWCC-
136 3100, World Precision Instruments, Sarasota, FL, USA; (Yuan et al., 2020)). The
137 absorption coefficient (Abs) of WSOC ~~was~~ were calculated according to formula S1 in
138 the Supporting Information (SI).

139 The total concentration and soluble fraction concentration of 14 trace elements
140 (i.e., Ti, V, Cr, Mn, Fe, Co, Ni, Cu, Zn, As, Sr, Cd, Ba, and Pb) were quantified by an
141 inductively coupled plasma mass spectrometer (ICP-MS, 7700x, Agilent Technologies,
142 USA), and the details are shown in the SI. For soluble fraction concentration analysis,
143 a punch of filter (47 mm diameter) was extracted with ultrapure water and then
144 centrifuged from residues. For total concentration analysis, another [47 mm diameter](#)

145 filter of the same sample with same size was used and ~~digestion after added of digested~~
146 with 10 mL HNO₃ and 1 mL HF at 180 °C for 12 h. The extracts were then heated and
147 concentrated to ~ 0.1 mL, and diluted to 5 mL with 2% HNO₃. Afterwards, the
148 diluents were filtered with a 0.22 µm PTFE pore syring filter and stored in a freezer
149 (-4 °C) until further ICP-MS analysis.

150 The concentrations of organic markers (including levoglucosan, mannosan,
151 galactosan, hopanes (including 17α(H)-22,29,30-trisnorhopane, 17α(H),21β(H)-30-
152 norhopane, 17β(H),21α(H)-30-norhopane, 17β(H),21α(H)-hopane, 17β(H),21α(H)-
153 hopane and 17β(H),21α(H)-hopane), picene, phthalic acid, isophthalic acid and
154 terephthalic acid) and light-absorbing NACs (including 4-nitrophenol (4NP), 2-
155 methyl-4-nitrophenol (2M4NP), 3-methyl-4-nitrophenol (3M4NP), 4-nitrocatechol
156 (4NC), 3-methyl-5-nitrocatechol (3M5NC), 4-methyl-5-nitrocatechol (4M5NC) and
157 4-nitro-1-naphthol (4N1N)) were determined by a gas chromatograph–mass
158 spectrometer (GC-MS; Agilent Technologies, Santa Clara, CA, USA) following the
159 method described elsewhere (Wang et al., 2020a), and more details about the analysis
160 can be found in SI. All of the results reported in this study were corrected for blanks.

161 **2.3 Oxidative potential**

162 The DTT assay was applied to determine the oxidative potential of water-soluble
163 components in PM_{2.5} according to the method by Gao et al. (2017). In brief, a quarter
164 of a 47 mm filter was ultrasonically extracted with 5 mL ultrapure water for 30 min
165 and then filtered with a 0.45 µm PVDF pore syring filter to remove insoluble
166 substances. Several studies have shown that ultrasonic treatment of samples can lead
167 to an increase in its OP values (Miljevic et al., 2014; Jiang et al., 2019), however,
168 there was also a study showed that the difference in OP values of water-soluble PM_{2.5}
169 measured by DTT assay was little for samples extracted by ultrasonic and shaking
170 (Gao et al., 2017). Consistent with the extraction methods of organic markers and
171 trace elements analysis, ultrasonic method was used to extract samples for DTT
172 analysis. Afterwards, 0.5 mL of the extract was mixed with 1 mL of potassium
173 phosphate buffer (pH = 7.4) and 0.5 mL of 2 mM DTT in a brown vial, and then

174 placed in a water bath at 37 °C. Then, 20 µL of this mixture was taken at designated
175 time intervals (2, 7, 13, 20, and 28 min) and mixed with 1 mL trichloroacetic acid
176 (TCA; 1% w/v) in another brown vial to terminate the reaction. Then, 0.5 mL of 5,5'-
177 dithiobis-(2-nitrobenzoic acid) (DTNB; 2.5 µM) and 2 mL of tris buffer (pH = 8.9)
178 were added to form 2-nitro-5-thiobenzonic acid (TNB) which has light absorption at
179 412 nm. Finally, the absorption of TNB was measured by a LWCC-UV-Vis. The DTT
180 consumption rate was quantified by the remaining DTT concentration at different
181 reaction times. Daily solution blanks and filter blanks were analyzed in parallel with
182 samples to evaluate the consistency of the system performance. Ambient samples
183 were corrected for filter blank. The DTT activities were normalized by the volume of
184 sampled air (DTT_v , $\text{nmol min}^{-1} \text{m}^{-3}$) and the mass concentration of $\text{PM}_{2.5}$ (DTT_m ,
185 $\text{pmol min}^{-1} \mu\text{g}^{-1}$).

186 Considering that for samples with significant contributions from species whose
187 DTT response is non-linear related to $\text{PM}_{2.5}$ mass (e.g., Cu, Mn), the DTT_m value
188 depends on the concentration of $\text{PM}_{2.5}$ in the extraction solution (Charrier et al., 2016).
189 The response of DTT_m to $\text{PM}_{2.5}$ concentration in the extraction solution was analyzed
190 using sample with high concentrations of soluble Cu and Mn (Figure S2). In the range
191 of $\text{PM}_{2.5}$ concentrations less than $150 \mu\text{g mL}^{-1}$, the DTT_m response was greatly
192 affected by $\text{PM}_{2.5}$ concentrations, however, when the concentrations of $\text{PM}_{2.5}$ in the
193 extract were greater than $150 \mu\text{g mL}^{-1}$, the DTT_m response changed little ($< 12\%$)
194 with the increase of $\text{PM}_{2.5}$ concentrations. In this study, the concentrations of $\text{PM}_{2.5}$ in
195 the extraction solution of most samples from the two sites were greater than $150 \mu\text{g}$
196 mL^{-1} (ranged from 78.7 to $748.7 \mu\text{g mL}^{-1}$, with average values of 408.9 ± 164.1 and
197 $206.6 \pm 95.0 \mu\text{g mL}^{-1}$ in the south and north, respectively), therefore, the difference in
198 $\text{PM}_{2.5}$ concentrations in different sample extracts should had a relatively small impact
199 on the difference in DTT_m values of the samples. This study did not consider the
200 impact of metal precipitation in phosphate matrix on the measured DTT values, as
201 there is no a straightforward method to correct the artifacts caused by this
202 phenomenon (Yalamanchili et al., 2023).

203 **2.4 Source apportionment**

204 The sources of DTT activities were identified and quantified using PMF model
205 implemented by the multilinear engine (ME-2; (Paatero, 1997)) following the method
206 described in our previous studies (Huang et al., 2014; Yuan et al., 2020). A total of 62
207 samples and 23 species were input into PMF model. The number of samples is higher
208 than the number of species, and approaching the ratio of at least 3:1 proposed by Belis
209 et al. (2019). The input data include species concentration (including DTT_v, 14 trace
210 elements and 8 organic markers) and uncertainties. The species-specific uncertainties
211 were calculated following Liu et al. (2017). More details are described in SI (PMF
212 analysis).

213

214 **3 Results and discussion**

215 **3.1 DTT activity and concentrations of water-soluble PM_{2.5} components**

216 Figure 1 shows the daily variation of DTT activity, light absorption of WSOC at
217 wavelength 365 nm (Abs₃₆₅), together with the concentrations of PM_{2.5}, WSOC,
218 NACs and total elements in the south and north of Beijing. Their average values are
219 shown in Table S1. Generally, the average values of PM_{2.5}, WSOC, Abs₃₆₅, NACs and
220 total elements were higher in the south than in the north. Specifically, the
221 concentrations of PM_{2.5} and WSOC in the south ($122.3 \pm 48.9 \mu\text{g m}^{-3}$ and 8.1 ± 5.0
222 $\mu\text{gC m}^{-3}$, respectively) were both about two times higher than that in the north ($62.3 \pm$
223 $27.9 \mu\text{g m}^{-3}$ and $4.0 \pm 2.0 \mu\text{gC m}^{-3}$, respectively), indicating that the proportion of
224 WSOC in PM_{2.5} was similar in the south and north. However, the Abs₃₆₅ in the south
225 was about three times that in the north, indicating that the chemical composition of
226 WSOC was different between the south and north. Previous studies have reported that
227 NACs are the main water-soluble light-absorbing organic compounds (also known as
228 brown carbon, BrC) of PM_{2.5} (Lin et al., 2017; Huang et al., 2020; Li et al., 2020). For
229 the 7 NACs quantified in this study, the total concentration of nitrophenols (4NP,
230 2M4NP and 3M4NP), nitrocatechols (4NC, 3M5NC and 4M5NC), and 4N1N in the
231 south ($108.5 \pm 72.9 \text{ ng m}^{-3}$, $118.5 \pm 91.5 \text{ ng m}^{-3}$ and $12.4 \pm 8.2 \text{ ng m}^{-3}$, respectively)

232 was about three, five and four times, respectively, those in the north ($35.5 \pm 21.7 \text{ ng}$
233 m^{-3} , $24.1 \pm 30.4 \text{ ng m}^{-3}$ and $3.1 \pm 3.0 \text{ ng m}^{-3}$, respectively). These results indicate that
234 the sources and emission strength of water-soluble organic compounds were different
235 in the south and north of Beijing, suggesting the different contribution of water-
236 soluble organic compounds to DTT activity. The concentration trend of elements was
237 also different between the south and north of Beijing, with $\text{Fe} > \text{Zn} > \text{Ti} > \text{Mn} > \text{Cu} >$
238 $\text{Ba} > \text{Pb} > \text{Sr} > \text{Cr} > \text{As} > \text{V} > \text{Ni} > \text{Cd} > \text{Co}$ in the south, and $\text{Fe} > \text{Ti} > \text{Zn} > \text{Ba} >$
239 $\text{Mn} > \text{Pb} > \text{Cu} > \text{Cr} > \text{Sr} > \text{As} > \text{Ni} > \text{V} > \text{Cd} > \text{Co}$ in the north. It should be noted that
240 although the content of $\text{PM}_{2.5}$, WSOC and total elements measured in this study were
241 higher in the south than in the north, the average DTT_v value in the south (3.9 ± 0.9
242 $\text{nmol min}^{-1} \text{ m}^{-3}$) was comparable to that in the north ($3.5 \pm 1.2 \text{ nmol min}^{-1} \text{ m}^{-3}$),
243 meanwhile, the average DTT_m value was much higher (1.8 times) in the north ($65.3 \pm$
244 $27.6 \text{ pmol min}^{-1} \mu\text{g}^{-1}$) than in the south ($36.1 \pm 14.5 \text{ pmol min}^{-1} \mu\text{g}^{-1}$). The lower
245 DTT_m in the south than in the north may be due to ~~that~~ the increased $\text{PM}_{2.5}$ in the
246 south contain~~ing~~s more substances with no or little contribution to DTT activity, and
247 indicates that the intrinsic OP of water-soluble components of $\text{PM}_{2.5}$ was higher in the
248 north than in the south. The similar DTT_v values in the south and north indicate that
249 the exposure-relevant OP_{toxicity} of water-soluble components of $\text{PM}_{2.5}$ was
250 comparable in the two sites, and the water-soluble DTT_v was not consistent with the
251 content of water-soluble substances.

252 Figure 2 shows the comparison of water-soluble $\text{PM}_{2.5}$ DTT activity ~~DTT_v and~~
253 ~~DTT_m values~~ measured in this study with those measured in other regions of Asia
254 during similar periods. It can be seen that the DTT_v values measured in Beijing in this
255 study (~~Campbell et al., 2021; Oh et al., 2023; this study~~) were lower than that in
256 Jinzhou, Tianjin, Yantai, and Shanghai in China, Lahore and Peshawar in Pakistan,
257 and Delhi in India (Liu et al., 2018; Ahmad et al., 2021; Puthussery et al., 2022; Wu et
258 al., 2022a), higher than that in Xi'an, Nanjing, Hangzhou, Guangzhou, and Shenzhen
259 in China, ~~and Gwangju in Korea~~ (Wang et al., 2019; Wang et al., 2020b; Ma et al.,
260 2021; Yu et al., 2022c; ~~Oh et al., 2023~~; Xing et al., 2023), and comparable with that in

261 Ningbo, China (Chen et al., 2022). Different from DTT_v , the DTT_m value measured in
262 NCNT in Beijing was similar with that in Jinzhou, Tianjin, Yantai, Shanghai and
263 Ningbo in China (Liu et al., 2018; Chen et al., 2022; Wu et al., 2022a), and higher
264 than that in other regions. The differences in water-soluble DTT activity of $PM_{2.5}$
265 DTT_v and DTT_m values in different regions ~~reflect the regional differences in $PM_{2.5}$~~
266 ~~exposure risk and intrinsic toxicity, which~~ can be explained by the differences in
267 chemical composition, sources and atmospheric formation processes (Tong et al.,
268 2017; Wong et al., 2019; Daellenbach et al., 2020; Wang et al., 2020b; Cao et al.,
269 2021). For example, Cao et al. (2021) reported the water-soluble DTT activity of
270 $PM_{2.5}$ from biomass and coal burning emissions in China, and the average value of
271 biomass burning ($4.5-7.4 \text{ pmol min}^{-1} \mu\text{g}^{-1}$) was much higher than that of coal burning
272 ($0.5-2.1 \text{ pmol min}^{-1} \mu\text{g}^{-1}$). Tuet et al. (2017) measured the water-soluble DTT activity
273 of SOA generated under different precursors and reaction conditions, with SOA from
274 naphthalene photooxidation under $RO_2 + NO$ -dominant dry reaction conditions had
275 the highest DTT activity.

276 **3.2 Correlation between DTT activity and water-soluble $PM_{2.5}$ components**

277 Figure 3 shows the correlations of DTT_v with $PM_{2.5}$, WSOC and Abs_{365} in the
278 south and north of Beijing. It can be seen that the correlation coefficient between
279 DTT_v and $PM_{2.5}$ was moderate in both the south ($r = 0.42$) and north ($r = 0.45$),
280 indicating that the toxicity of particles can not be evaluated solely by the total $PM_{2.5}$
281 concentration. The correlations between DTT_v with WSOC and Abs_{365} were strong in
282 the north (r of 0.69 and 0.70, respectively), while relatively weak in the south (r of
283 0.41 and 0.40, respectively). The high correlations between DTT_v with WSOC and
284 Abs_{365} in the north of Beijing qualitatively agree~~are coincide~~ with previous studies in
285 Xi'an, China and Atlanta, United States (Verma et al., 2012; Chen et al., 2019), and
286 suggest that water-soluble organic matter, especially BrC, has a significant
287 contribution to DTT consumption in the north. Light-absorbing BrC typically has
288 conjugated electrons, making it more likely to transport electrons for catalytic
289 reactions, thereby contributing to DTT activity (Chen et al., 2019; Wu et al., 2022).

290 Further, in the north, the DTT_v was closely related to the concentrations of NACs (r of
291 0.57 to 0.79) (Figure S32), suggesting that NACs ~~mayeould~~ be important contributors
292 to DTT consumption. Feng et al. (2022) reported the positive correlations between
293 NACs and biomarkers in saliva and urine (interleukin-6 and 8-hydrox-2'-
294 deoxyguanosine). Zhang et al. (2023) also reported that NACs are major
295 proinflammatory components in organic aerosols, contributing about 24% of the
296 interleukin-8 response of all compounds detected by Fourier transform ion cyclotron
297 resonance mass spectrometry (FT-ICR-MS) in electrospray ionization negative mode
298 (ESI-). Certainly, it may also be other substances related to NACs that contribute to
299 the DTT activity, including those not detected in this study, driving the good
300 correlation between NACs and DTT_v in the north of Beijing, which is worth studying
301 in the future.

302 The correlation coefficients between DTT_v and 14 trace elements are shown in
303 Figure 4. Generally, the correlations between DTT_v and soluble elements were higher
304 than that between DTT_v and total elements in both the south and north of Beijing;
305 ~~suggesting that the consumption of DTT from elements depend primarily on its~~
306 ~~soluble fraction instead of their total content.~~ For soluble elements, in the south, the
307 DTT_v showed positive correlations with Mn, Fe, Cr, Co, As and Pb (r > 0.5), while in
308 the north, it exhibited strong positive correlations with Mn, Co, Ni, Zn, As, Cd and Pb
309 (r > 0.7), indicating the different sources of DTT_v in the south and north of Beijing. It
310 is worth noting that the concentrations of all soluble elements were higher in the south
311 than in the north (Figure S43), while the correlation between DTT_v and most soluble
312 elements was lower in the south than in the north (Figure 4). The high correlations
313 between DTT_v and soluble elements in the north of Beijing suggests that soluble
314 elements also had significant contribution to DTT consumption. The low correlations
315 between DTT_v and soluble elements in the south of Beijing may be due to the
316 nonlinear relationship between DTT consumption and elements concentrations
317 (Charrier and Anastasio, 2012; Wu et al., 2022a).

318 In addition to being associated with individual water-soluble species, the

319 interaction between metal and organic compounds also affects the consumption of
320 DTT (Xiong et al., 2017; Wu et al., 2022b), with both synergistic and antagonistic
321 effects. For example, Wu et al. (2022b) measured the DTT consumption of Fe(III) and
322 Cu(II) interacting with 1,4-naphthoquinone, 9,10-phenanthraquinone, citric acid, and
323 4-nitrocatechol, respectively. Their results showed that Cu(II) had antagonistic effects
324 in interacting with most organics except for citric acid, and Fe(III) had an additive
325 effect on DTT consumption of 1,4-naphthoquinone and citric acid, while it had an
326 antagonistic effect on 1,4-naphthoquinone and 9,10-phenanthraquinone. Due to the
327 complex composition of water-soluble organic aerosols, the knowledge about the
328 effects of organics and metal-organic interactions on DTT activity are still limited,
329 especially the effects of BrC chromophores and their interactions with metals.

330 **3.3 Sources of DTT activity**

331 ~~The PMF model was applied to quantify the sources of DTT_v in the south and the~~
332 ~~north of Beijing, which was widely used for the source apportionment of PM_{2.5}-OP~~
333 ~~(Liu et al., 2018; Shen et al., 2022; Cui et al., 2023). The input species include DTT_v,~~
334 ~~soluble elements, and~~This study analyzed eight organic markers (including
335 levoglucosan, mannosan, and galactosan for biomass burning, hopanes for vehicle
336 emissions, picene for coal combustion, and phthalic acid, isophthalic acid and
337 terephthalic acid for secondary formation) to help identify the sources of DTT activity.
338 The correlation coefficients between DTT_v and organic markers are shown in Figure
339 S54. In the south, levoglucosan, mannosan, galactosan, and hopanes had moderate
340 correlation with DTT_v (r of 0.41 to 0.48); phthalic acid, isophthalic acid and
341 terephthalic acid had low to moderate correlation with DTT_v (r of 0.28 to 0.54);
342 picene had low correlation with DTT_v (r of 0.21). These results suggest that biomass
343 burning and vehicle emissions could have significant contribution to water-soluble
344 PM_{2.5} OP in the south. In the north, hopanes had the highest correlation with DTT_v (r
345 = 0.70), indicating that vehicle emissions could have an important contribution.
346 Levoglucosan, mannosan, galactosan, phthalic acid, isophthalic acid, terephthalic acid,
347 and picene had moderate to high correlations with DTT_v in the north, suggesting that

348 biomass and coal burning, and secondary formation may also have certain
349 contribution to water-soluble PM_{2.5} OP.

350 To further quantify the sources of DTT activity in the south and the north of
351 Beijing, the PMF model, which was widely used for the source apportionment of
352 PM_{2.5} OP (Liu et al., 2018; Shen et al., 2022; Cui et al., 2023), was applied. The input
353 species include DTT_v, soluble elements and organic markers, and five to seven factors
354 were examined. Due to the oil factor mixed with vehicle emissions factor in the five-
355 factor solution, and there was no new reasonable factor when increasing the factor
356 number to seven in the PMF analysis (Figure S6). Finally, ~~Six~~six factors were
357 resolved and quantified using PMF model in the south and north of Beijing, including
358 biomass burning, coal burning, traffic-related, dust, oil combustion, and secondary
359 formation, and the profiles of these sources are shown in Figure S7. Factor 1 is
360 characterized by high contribution of levoglucosan, mannosan, and galactosan, mainly
361 from biomass burning (Huang et al., 2014; Chow et al., 2022). The DTT activity of
362 biomass burning organic aerosol was measured by Wong et al. (2019), which was 48
363 ± 6 pmol min⁻¹ μg⁻¹ of WSOC. Liu et al. (2018) quantified the sources of DTT_v in
364 coastal cities (Jinzhou, Tianjin, and Yantai) in China with PMF model and multiple
365 linear regression method, and the results showed that biomass burning contributed
366 27.8% on average in winter. Factor 2 exhibits a large fraction of picene, Zn, Mn,
367 Cd, As, and Pb, which is considered to be coal burning (Huang et al., 2014; Huang et
368 al., 2018). Joo et al. (2018) measured the DTT activity of PM_{2.5} emitted from coal
369 combustion at different temperatures, with the highest values of 26.2 ± 20.5 pmol
370 min⁻¹ μg⁻¹ and 0.10 ± 0.06 nmol min⁻¹ m⁻³ occurring at 550 °C. Factor 3 is identified
371 as traffic-related emissions, which is characterized by the higher loading of hopanes,
372 Ba, Sr, Cu and Ni (Huang et al., 2018; Chow et al., 2022). Vreeland et al. (2017)
373 measured the DTT activity of PM_{2.5} emitted by side street and highway vehicles in
374 Atlanta, with values of 0.78 ± 0.60 nmol min⁻¹ m⁻³ and 1.08 ± 0.60 nmol min⁻¹ m⁻³,
375 respectively. Ting et al. (2023) reported that the DTT activity of PM_{2.5} from vehicle
376 emissions in Ziqing tunnel in Taiwan, China, was 0.15-0.46 nmol min⁻¹ m⁻³. Factor 4,

377 secondary formation, which is identified by high levels of phthalic acid, isophthalic
378 acid, and terephthalic acid (Al-Naiema and Stone, 2017; Wang et al., 2020a). Verma et
379 al. (2014) reported that secondary formation contributed about 30% to the water-
380 soluble DTT activity of PM_{2.5} in urban Atlanta. It is worth noting that the DTT
381 activity of SOA generated from different precursors is different (Tuet et al., 2017;
382 Tong et al., 2018). For example, the DTT activity of SOA from naphthalene was
383 higher than that from isoprene (Tuet et al., 2017; Tong et al., 2018). Factor 5 is
384 dominated by crustal elements Fe and Ti, mainly from dust (Huang et al., 2018). The
385 DTT activity of atmospheric particulate matter during dust periods were reported in
386 previous studies (Chirizzi et al., 2017; Khoshnamvand et al., 2023) and it has a low
387 contribution in this study. Factor 6 is identified as oil combustion because of the high
388 levels of V and Ni (Moreno et al., 2011; Minguillón et al., 2014; Huang et al., 2018).

389 The source contributions of DTT_v in the south and north of Beijing are shown in
390 Figure 5, exhibiting obvious **districtregional** differences. In the south, traffic-related
391 emissions (39.1%) and biomass burning (25.2%) had the most contribution to DTT_v,
392 followed by secondary formation (17.2%), coal burning (15%), dust (2%), and oil
393 combustion (1.5%). In the north, traffic-related emissions (51.6%) had the highest
394 contribution to DTT_v, followed by coal burning (19.9%), secondary formation (13%),
395 biomass burning (8.4%), oil combustion (4.1%), and dust (3%). The large
396 **districtregional** differences in sources of DTT_v of water-soluble PM_{2.5} call for more
397 research on the relationship between sources, chemical composition, formation
398 processes and OP of PM_{2.5}.

399

400 **4 Conclusions**

401 In this study, the water-soluble OP of ambient PM_{2.5} collected in winter in the
402 south and north of Beijing were quantified, together with the concentration and light
403 absorption of WSOC, and concentrations of 7 light-absorbing NACs and 14 trace
404 elements. The average DTT_v value was comparable in the south ($3.9 \pm 0.9 \text{ nmol min}^{-1}$
405 m^{-3}) and north ($3.5 \pm 1.2 \text{ nmol min}^{-1} \text{ m}^{-3}$), while the DTT_m was higher in the north

406 (65.3 ± 27.6 pmol min⁻¹ μg⁻¹) than in the south (36.1 ± 14.5 pmol min⁻¹ μg⁻¹),
407 indicating that the PM_{2.5}-exposure-relevant toxicityOP of water-soluble components
408 of PM_{2.5} was similar in the two sites and that the PM_{2.5}-intrinsic toxicityOP of water-
409 soluble components of PM_{2.5} was higher in the north than in the south. The correlation
410 between DTT_v and soluble elements was higher than that between DTT_v and total
411 elements in both the south and north. In the north, the DTT_v was strongly correlated
412 with soluble Mn, Co, Ni, Zn, As, Cd and Pb (r > 0.7), and in the south it positively
413 correlated with Mn, Fe, Cr, Co, As and Pb (r > 0.5). In addition, in the north the DTT_v
414 was also positively correlated with WSOC, Abs₃₆₅ and NACs (r of 0.56 to 0.79),
415 while in the south it was weakly correlated (r ≤ 0.4). These results indicate that in the
416 north trace elements and water-soluble organic compounds, especially BrC
417 chromophores, both had significant contributions to DTT consumption, and in the
418 south the consumption of DTT may be mainly from trace elements. Six sources of
419 DTT_v were resolved with the PMF model, including biomass burning, coal burning,
420 traffic-related, dust, oil combustion, and secondary formation. On average, traffic-
421 related emissions (39.1%) and biomass burning (25.2%) were the major contributors
422 of DTT_v in the south, and traffic-related emissions (51.6%) was the predominated
423 source in the north. The differences in DTT_v sources in the south and north of Beijing
424 suggest that the relationship between source emissions and atmospheric processes and
425 PM_{2.5} OP deserve further exploration in order to better understand the regional
426 differences of health impacts of PM_{2.5}.

427

428

429

430 **Date availability.** Raw data used in this study can be obtained from the following
431 open link: <https://doi.org/10.5281/zenodo.10791126> (Yuan et al., 2024). It is also
432 available on request by contacting the corresponding author.

433

434 **Supplement.** The Supplement related to this article is available online.

435

436 **Author contributions.** RJH designed the study. Data analysis was done by WY, CL,
437 LY, HY and RJH. WY, CL, LY, HY and RJH interpreted data, prepared the display
438 items and wrote the manuscript. All authors commented on and discussed the
439 manuscript.

440

441 **Competing interests.** The authors declare that they have no conflict of interest.

442

443 **Acknowledgements.** We are very grateful to the National Natural Science Foundation
444 of China (NSFC) under Grant No. 41925015, the Strategic Priority Research Program
445 of Chinese Academy of Sciences (XDB40000000), the Key Research Program of
446 Frontier Sciences from the Chinese Academy of Sciences (ZDBS-LY-DQC001), the
447 New Cornerstone Science Foundation through the XPLOER PRIZE, and the
448 Postdoctoral Fellowship Program of CPSF (no. GZC20232628) supported this study.

449

450 **Financial support.** This work was supported by the National Natural Science
451 Foundation of China (NSFC) under Grant No. 41925015, the Strategic Priority
452 Research Program of Chinese Academy of Sciences (XDB40000000), the Key
453 Research Program of Frontier Sciences from the Chinese Academy of Sciences
454 (ZDBS-LY-DQC001), the New Cornerstone Science Foundation through the
455 XPLOER PRIZE, and the Postdoctoral Fellowship Program of CPSF (no.
456 GZC20232628).

457

458

459 **References**

460 Ahmad, M., Yu, Q., Chen, J., Cheng, S., Qin, W., and Zhang, Y.: Chemical
461 characteristics, oxidative potential, and sources of PM_{2.5} in wintertime in
462 Lahore and Peshawar, Pakistan, *J. Environ. Sci.*, 102, 148-158,
463 10.1016/j.jes.2020.09.014, 2021.

464 Al-Naiema, I. M. and Stone, E. A.: Evaluation of anthropogenic secondary organic
465 aerosol tracers from aromatic hydrocarbons, *Atmos. Chem. Phys.*, 17, 2053-
466 2065, 10.5194/acp-17-2053-2017, 2017.

467 An, Z., Huang, R. J., Zhang, R., Tie, X., Li, G., Cao, J., Zhou, W., Shi, Z., Han, Y., Gu,
468 Z., and Ji, Y.: Severe haze in northern China: A synergy of anthropogenic
469 emissions and atmospheric processes, *Proc. Natl. Acad. Sci. U. S. A.*, 116,
470 8657-8666, 10.1073/pnas.1900125116, 2019.

471 Bates, J. T., Fang, T., Verma, V., Zeng, L., Weber, R. J., Tolbert, P. E., Abrams, J. Y.,
472 Sarnat, S. E., Klein, M., Mulholland, J. A., and Russell, A. G.: Review of
473 Acellular Assays of Ambient Particulate Matter Oxidative Potential: Methods
474 and Relationships with Composition, Sources, and Health Effects, *Environ.*
475 *Sci. Technol.*, 53, 4003-4019, 10.1021/acs.est.8b03430, 2019.

476 Belis, C., Larsen, B. R., Amato, F., Haddad, I. El, Favez, O., Harrison, R. M., Hopke,
477 P. K., Nava, S., Paatero, P., Prévôt, A., Quass, U., Vecchi, R., and Viana, M.:
478 European Guide on Air Pollution Source Apportionment with Receptor
479 Models, JRC References Report, March, 88, 1-170,
480 <https://doi.org/10.2788/9307>, 2019.

481 Burnett, R., Chen, H., Szyszkowicz, M., Fann, N., Hubbell, B., Pope, C. A., 3rd, Apte,
482 J. S., Brauer, M., Cohen, A., Weichenthal, S., Coggins, J., Di, Q., Brunekreef,
483 B., Frostad, J., Lim, S. S., Kan, H., Walker, K. D., Thurston, G. D., Hayes, R.
484 B., Lim, C. C., Turner, M. C., Jerrett, M., Krewski, D., Gapstur, S. M., Diver,
485 W. R., Ostro, B., Goldberg, D., Crouse, D. L., Martin, R. V., Peters, P., Pinault,
486 L., Tjepkema, M., van Donkelaar, A., Villeneuve, P. J., Miller, A. B., Yin, P.,
487 Zhou, M., Wang, L., Janssen, N. A. H., Marra, M., Atkinson, R. W., Tsang, H.,
488 Quoc Thach, T., Cannon, J. B., Allen, R. T., Hart, J. E., Laden, F., Cesaroni, G.,
489 Forastiere, F., Weinmayr, G., Jaensch, A., Nagel, G., Concin, H., and Spadaro,
490 J. V.: Global estimates of mortality associated with long-term exposure to
491 outdoor fine particulate matter, *Proc. Natl. Acad. Sci. U. S. A.*, 115, 9592-9597,
492 10.1073/pnas.1803222115, 2018.

493 Calas, A., Uzu, G., Kelly, F. J., Houdier, S., Martins, J. M. F., Thomas, F., Molton, F.,
494 Charron, A., Dunster, C., Oliete, A., Jacob, V., Besombes, J.-L., Chevrier, F.,
495 and Jaffrezo, J.-L.: Comparison between five acellular oxidative potential
496 measurement assays performed with detailed chemistry on PM₁₀ samples from
497 the city of Chamonix (France), *Atmos. Chem. Phys.*, 18, 7863-7875,
498 10.5194/acp-18-7863-2018, 2018.

499 Campbell, S. J., Wolfer, K., Utinger, B., Westwood, J., Zhang, Z. H., Bukowiecki, N.,
500 Steimer, S. S., Vu, T. V., Xu, J., Straw, N., Thomson, S., Elzein, A., Sun, Y.,
501 Liu, D., Li, L., Fu, P., Lewis, A. C., Harrison, R. M., Bloss, W. J., Loh, M.,
502 Miller, M. R., Shi, Z., and Kalberer, M.: Atmospheric conditions and
503 composition that influence PM_{2.5} oxidative potential in Beijing, China, *Atmos.*
504 *Chem. Phys.*, 21, 5549-5573, 10.5194/acp-21-5549-2021, 2021.

505 Cao, T., Li, M., Zou, C., Fan, X., Song, J., Jia, W., Yu, C., Yu, Z., and Peng, P. a.:
506 Chemical composition, optical properties, and oxidative potential of water-
507 and methanol-soluble organic compounds emitted from the combustion of
508 biomass materials and coal, *Atmos. Chem. Phys.*, 21, 13187-13205,
509 10.5194/acp-21-13187-2021, 2021.

510 Charrier, J. G. and Anastasio, C.: On dithiothreitol (DTT) as a measure of oxidative
511 potential for ambient particles: evidence for the importance of soluble
512 transition metals, *Atmos. Chem. Phys.*, 12, 9321-9333, 10.5194/acp-12-9321-
513 2012, 2012.

514 [Charrier, J. G., McFall, A. S., Vu, K. K.-T., Baroi, J., Olea, C., Hasson, A., and](#)
515 [Anastasio, C.: A Bias in the “Mass-Normalized” DTT Response-An Effect of](#)
516 [Non-Linear Concentration Response Curves for Copper and Manganese,](#)
517 [Atmos. Environ., 144, 325-334, 2016.](#)

518 Chen, K., Xu, J., Famiyeh, L., Sun, Y., Ji, D., Xu, H., Wang, C., Metcalfe, S. E., Betha,
519 R., Behera, S. N., Jia, C., Xiao, H., and He, J.: Chemical constituents, driving
520 factors, and source apportionment of oxidative potential of ambient fine
521 particulate matter in a Port City in East China, *J. Hazard. Mater.*, 440,

522 10.1016/j.jhazmat.2022.129864, 2022.

523 Chen, Q., Wang, M., Wang, Y., Zhang, L., Li, Y., and Han, Y.: Oxidative Potential of
524 Water-Soluble Matter Associated with Chromophoric Substances in PM_{2.5}
525 over Xi'an, China, *Environ. Sci. Technol.*, 53, 8574-8584,
526 10.1021/acs.est.9b01976, 2019.

527 Chirizzi, D., Cesari, D., Guascito, M. R., Dinoi, A., Giotta, L., Donato, A., and
528 Contini, D.: Influence of Saharan dust outbreaks and carbon content on
529 oxidative potential of water-soluble fractions of PM_{2.5} and PM₁₀, *Atmos.*
530 *Environ.*, 163, 1-8, 10.1016/j.atmosenv.2017.05.021, 2017.

531 Chow, W. S., Huang, X. H. H., Leung, K. F., Huang, L., Wu, X., and Yu, J. Z.:
532 Molecular and elemental marker-based source apportionment of fine
533 particulate matter at six sites in Hong Kong, China, *Sci. Total Environ.*, 813,
534 152652, 10.1016/j.scitotenv.2021.152652, 2022.

535 Chowdhury, P. H., He, Q., Carmieli, R., Li, C., Rudich, Y., and Pardo, M.: Connecting
536 the Oxidative Potential of Secondary Organic Aerosols with Reactive Oxygen
537 Species in Exposed Lung Cells, *Environ. Sci. Technol.*, 53, 13949-13958,
538 10.1021/acs.est.9b04449, 2019.

539 Cui, Y., Zhu, L., Wang, H., Zhao, Z., Ma, S., and Ye, Z.: Characteristics and Oxidative
540 Potential of Ambient PM_{2.5} in the Yangtze River Delta Region: Pollution Level
541 and Source Apportionment, *Atmosphere*, 14, 10.3390/atmos14030425, 2023.

542 Daellenbach, K. R., Uzu, G., Jiang, J., Cassagnes, L. E., Leni, Z., Vlachou, A.,
543 Stefanelli, G., Canonaco, F., Weber, S., Segers, A., Kuenen, J. J. P., Schaap, M.,
544 Favez, O., Albinet, A., Aksoyoglu, S., Dommen, J., Baltensperger, U., Geiser,
545 M., El Haddad, I., Jaffrezo, J. L., and Prevot, A. S. H.: Sources of particulate-
546 matter air pollution and its oxidative potential in Europe, *Nature*, 587, 414-419,
547 10.1038/s41586-020-2902-8, 2020.

548 Fan, X., Li, M., Cao, T., Cheng, C., Li, F., Xie, Y., Wei, S., Song, J., and Peng, P. a.:
549 Optical properties and oxidative potential of water- and alkaline-soluble
550 brown carbon in smoke particles emitted from laboratory simulated biomass

551 burning, *Atmos. Environ.*, 194, 48-57, 10.1016/j.atmosenv.2018.09.025, 2018.

552 Fang, T., Verma, V., Bates, J. T., Abrams, J., Klein, M., Strickland, M. J., Sarnat, S. E.,
553 Chang, H. H., Mulholland, J. A., Tolbert, P. E., Russell, A. G., and Weber, R. J.:
554 Oxidative potential of ambient water-soluble PM_{2.5} in the southeastern United
555 States: contrasts in sources and health associations between ascorbic acid (AA)
556 and dithiothreitol (DTT) assays, *Atmos. Chem. Phys.*, 16, 3865-3879,
557 10.5194/acp-16-3865-2016, 2016.

558 Feng, R., Xu, H., Gu, Y., Wang, Z., Han, B., Sun, J., Liu, S., Lu, H., Ho, S. S. H.,
559 Shen, Z., and Cao, J.: Variations of Personal Exposure to Particulate Nitrated
560 Phenols from Heating Energy Renovation in China: The First Assessment on
561 Associated Toxicological Impacts with Particle Size Distributions, *Environ.*
562 *Sci. Technol.*, 56, 3974–3983, 2022.

563 Gao, D., Fang, T., Verma, V., Zeng, L., and Weber, R. J.: A method for measuring total
564 aerosol oxidative potential (OP) with the dithiothreitol (DTT) assay and
565 comparisons between an urban and roadside site of water-soluble and total OP,
566 *Atmos. Meas. Tech.*, 10, 2821-2835, 10.5194/amt-10-2821-2017, 2017.

567 Hecobian, A., Zhang, X., Zheng, M., Frank, N., Edgerton, E. S., and Weber, R. J.:
568 Water-Soluble Organic Aerosol material and the light-absorption
569 characteristics of aqueous extracts measured over the Southeastern United
570 States, *Atmos. Chem. Phys.*, 10, 5965-5977, 10.5194/acp-10-5965-2010, 2010.

571 Ho, K. F., Ho, S. S. H., Huang, R.-J., Liu, S. X., Cao, J.-J., Zhang, T., Chuang, H.-C.,
572 Chan, C. S., Hu, D., and Tian, L.: Characteristics of water-soluble organic
573 nitrogen in fine particulate matter in the continental area of China, *Atmos.*
574 *Environ.*, 106, 252-261, 10.1016/j.atmosenv.2015.02.010, 2015.

575 Huang, R. J., Cheng, R., Jing, M., Yang, L., Li, Y., Chen, Q., Chen, Y., Yan, J., Lin, C.,
576 Wu, Y., Zhang, R., El Haddad, I., Prevot, A. S. H., O'Dowd, C. D., and Cao, J.:
577 Source-Specific Health Risk Analysis on Particulate Trace Elements: Coal
578 Combustion and Traffic Emission As Major Contributors in Wintertime
579 Beijing, *Environ. Sci. Technol.*, 52, 10967-10974, 10.1021/acs.est.8b02091,

580 2018.

581 Huang, R. J., Yang, L., Shen, J., Yuan, W., Gong, Y., Guo, J., Cao, W., Duan, J., Ni, H.,
582 Zhu, C., Dai, W., Li, Y., Chen, Y., Chen, Q., Wu, Y., Zhang, R., Dusek, U.,
583 O'Dowd, C., and Hoffmann, T.: Water-Insoluble Organics Dominate Brown
584 Carbon in Wintertime Urban Aerosol of China: Chemical Characteristics and
585 Optical Properties, *Environ. Sci. Technol.*, 54, 7836-7847,
586 10.1021/acs.est.0c01149, 2020.

587 Huang, R. J., Zhang, Y., Bozzetti, C., Ho, K. F., Cao, J. J., Han, Y., Daellenbach, K. R.,
588 Slowik, J. G., Platt, S. M., Canonaco, F., Zotter, P., Wolf, R., Pieber, S. M.,
589 Bruns, E. A., Crippa, M., Ciarelli, G., Piazzalunga, A., Schwikowski, M.,
590 Abbaszade, G., Schnelle-Kreis, J., Zimmermann, R., An, Z., Szidat, S.,
591 Baltensperger, U., El Haddad, I., and Prevot, A. S.: High secondary aerosol
592 contribution to particulate pollution during haze events in China, *Nature*, 514,
593 218-222, 10.1038/nature13774, 2014.

594 Jiang, H., Xie, Y., Ge, Y., He, H., and Liu, Y.: Effects of ultrasonic treatment on
595 dithiothreitol (DTT) assay measurements for carbon materials, *J. Environ. Sci.*,
596 84, 51–58, 2019.

597 Joo, H. S., Batmunkh, T., Borlaza, L. J. S., Park, M., Lee, K. Y., Lee, J. Y., Chang, Y.
598 W., and Park, K.: Physicochemical properties and oxidative potential of fine
599 particles produced from coal combustion, *Aerosol Sci. Technol.*, 52, 1134-
600 1144, 10.1080/02786826.2018.1501152, 2018.

601 Khoshnamvand, N., Nodehi, R. N., Hassanvand, M. S., and Naddafi, K.: Comparison
602 between oxidative potentials measured of water-soluble components in
603 ambient air PM₁ and PM_{2.5} of Tehran, Iran, *Air Qual. Atmos. Hlth.*, 16, 1311-
604 1320, 10.1007/s11869-023-01343-y, 2023.

605 Laskin, A., Laskin, J., and Nizkorodov, S. A.: Chemistry of atmospheric brown carbon,
606 *Chem. Rev.*, 115, 4335-4382, 10.1021/cr5006167, 2015.

607 Lelieveld, S., Wilson, J., Dovrou, E., Mishra, A., Lakey, P. S. J., Shiraiwa, M., Poschl,
608 U., and Berkemeier, T.: Hydroxyl Radical Production by Air Pollutants in

609 Epithelial Lining Fluid Governed by Interconversion and Scavenging of
610 Reactive Oxygen Species, *Environ. Sci. Technol.*, 55, 14069-14079,
611 10.1021/acs.est.1c03875, 2021.

612 Lin, P., Bluvshstein, N., Rudich, Y., Nizkorodov, S. A., Laskin, J., and Laskin, A.:
613 Molecular chemistry of atmospheric brown carbon inferred from a nationwide
614 biomass burning event, *Environ. Sci. Technol.*, 51, 11561–11570, 2017.

615 Liu, W., Xu, Y., Liu, W., Liu, Q., Yu, S., Liu, Y., Wang, X., and Tao, S.: Oxidative
616 potential of ambient PM_{2.5} in the coastal cities of the Bohai Sea, northern
617 China: Seasonal variation and source apportionment, *Environ. Pollut.*, 236,
618 514-528, 10.1016/j.envpol.2018.01.116, 2018.

619 [Liu, Y., Yan, C. Q., Ding, X., Wang, X. M., Fu, Q. Y., Zhao, Q. B., Zhang, Y. H., Duan,](#)
620 [Y. S., Qiu, X. H., and Zheng, M.: Sources and spatial distribution of](#)
621 [particulate polycyclic aromatic hydrocarbons in Shanghai, China, *Sci. Total*](#)
622 [Environ.](#), 584-585, 307-317, <https://doi.org/10.1016/j.scitotenv.2016.12.134>,
623 [2017.](#)

624 Ma, X., Nie, D., Chen, M., Ge, P., Liu, Z., Ge, X., Li, Z., and Gu, R.: The Relative
625 Contributions of Different Chemical Components to the Oxidative Potential of
626 Ambient Fine Particles in Nanjing Area, *Int. J. Environ. Res. Public Health*, 18,
627 2789, 10.3390/ijerph18062789, 2021.

628 [Miljevic, B., Hedayat, F., Stevanovic, S., Fairfull-Smith, K. E., Bottle, S. E., and](#)
629 [Ristovski, Z. D.: To sonicate or not to sonicate PM filters: reactive oxygen](#)
630 [species generation upon ultrasonic irradiation, *Aerosol. Sci. Technol.*, 48,](#)
631 [1276-1284, 2014.](#)

632 Minguillón, M. C., Cirach, M., Hoek, G., Brunekreef, B., Tsai, M., de Hoogh, K.,
633 Jedynska, A., Kooter, I. M., Nieuwenhuijsen, M., and Querol, X.: Spatial
634 variability of trace elements and sources for improved exposure assessment in
635 Barcelona, *Atmos. Environ.*, 89, 268-281, 10.1016/j.atmosenv.2014.02.047,
636 2014.

637 Moreno, T., Querol, X., Alastuey, A., Reche, C., Cusack, M., Amato, F., Pandolfi, M.,

638 Pey, J., Richard, A., Prévôt, A. S. H., Furger, M., and Gibbons, W.: Variations
639 in time and space of trace metal aerosol concentrations in urban areas and their
640 surroundings, *Atmos. Chem. Phys.*, 11, 9415-9430, 10.5194/acp-11-9415-2011,
641 2011.

642 Oh, S. H., Park, K., Park, M., Song, M., Jang, K. S., Schauer, J. J., Bae, G. N., and
643 Bae, M. S.: Comparison of the sources and oxidative potential of PM_{2.5} during
644 winter time in large cities in China and South Korea, *Sci. Total Environ.*, 859,
645 160369, 10.1016/j.scitotenv.2022.160369, 2023.

646 Paatero, P.: Least squares formation of robust non negative factor analysis,
647 *Chemometr. Intell. Lab.*, 37, 23-35, 1997.

648 Puthussery, J. V., Dave, J., Shukla, A., Gaddamidi, S., Singh, A., Vats, P., Salana, S.,
649 Ganguly, D., Rastogi, N., Tripathi, S. N., and Verma, V.: Effect of Biomass
650 Burning, Diwali Fireworks, and Polluted Fog Events on the Oxidative
651 Potential of Fine Ambient Particulate Matter in Delhi, India, *Environ. Sci.*
652 *Technol.*, 56, 14605-14616, 10.1021/acs.est.2c02730, 2022.

653 Shen, J., Taghvaei, S., La, C., Oroumijeh, F., Liu, J., Jerrett, M., Weichenthal, S., Del
654 Rosario, I., Shafer, M. M., Ritz, B., Zhu, Y., and Paulson, S. E.: Aerosol
655 Oxidative Potential in the Greater Los Angeles Area: Source Apportionment
656 and Associations with Socioeconomic Position, *Environ. Sci. Technol.*, 56,
657 17795-17804, 10.1021/acs.est.2c02788, 2022.

658 Ting, Y. C., Chang, P. K., Hung, P. C., Chou, C. C., Chi, K. H., and Hsiao, T. C.:
659 Characterizing emission factors and oxidative potential of motorcycle
660 emissions in a real-world tunnel environment, *Environ. Res.*, 234, 116601,
661 10.1016/j.envres.2023.116601, 2023.

662 Tong, H., Lakey, P. S. J., Arangio, A. M., Socorro, J., Kampf, C. J., Berkemeier, T.,
663 Brune, W. H., Poschl, U., and Shiraiwa, M.: Reactive oxygen species formed
664 in aqueous mixtures of secondary organic aerosols and mineral dust
665 influencing cloud chemistry and public health in the Anthropocene, *Faraday*
666 *Discuss.*, 200, 251-270, 10.1039/c7fd00023e, 2017.

667 Tong, H., Lakey, P. S. J., Arangio, A. M., Socorro, J., Shen, F., Lucas, K., Brune, W.
668 H., Poschl, U., and Shiraiwa, M.: Reactive Oxygen Species Formed by
669 Secondary Organic Aerosols in Water and Surrogate Lung Fluid, *Environ. Sci.*
670 *Technol.*, 52, 11642-11651, 10.1021/acs.est.8b03695, 2018.

671 Tuet, W. Y., Chen, Y., Xu, L., Fok, S., Gao, D., Weber, R. J., and Ng, N. L.: Chemical
672 oxidative potential of secondary organic aerosol (SOA) generated from the
673 photooxidation of biogenic and anthropogenic volatile organic compounds,
674 *Atmos. Chem. Phys.*, 17, 839-853, 10.5194/acp-17-839-2017, 2017.

675 Tuet, W. Y., Liu, F., de Oliveira Alves, N., Fok, S., Artaxo, P., Vasconcellos, P.,
676 Champion, J. A., and Ng, N. L.: Chemical Oxidative Potential and Cellular
677 Oxidative Stress from Open Biomass Burning Aerosol, *Environ. Sci. Technol.*
678 *Lett.*, 6, 126-132, 10.1021/acs.estlett.9b00060, 2019.

679 Verma, V., Fang, T., Xu, L., Peltier, R. E., Russell, A. G., Ng, N. L., and Weber, R. J.:
680 Organic aerosols associated with the generation of reactive oxygen species
681 (ROS) by water-soluble PM_{2.5}, *Environ. Sci. Technol.*, 49, 4646-4656,
682 10.1021/es505577w, 2015.

683 Verma, V., Rico-Martinez, R., Kotra, N., King, L., Liu, J., Snell, T. W., and Weber, R.
684 J.: Contribution of water-soluble and insoluble components and their
685 hydrophobic/hydrophilic subfractions to the reactive oxygen species-
686 generating potential of fine ambient aerosols, *Environ. Sci. Technol.*, 46,
687 11384-11392, 10.1021/es302484r, 2012.

688 Verma, V., Fang, T., Guo, H., King, L., Bates, J. T., Peltier, R. E., Edgerton, E.,
689 Russell, A. G., and Weber, R. J.: Reactive oxygen species associated with
690 water-soluble PM_{2.5} in the southeastern United States: spatiotemporal trends
691 and source apportionment, *Atmos. Chem. Phys.*, 14, 12915-12930,
692 10.5194/acp-14-12915-2014, 2014.

693 Vreeland, H., Weber, R., Bergin, M., Greenwald, R., Golan, R., Russell, A. G., Verma,
694 V., and Sarnat, J. A.: Oxidative potential of PM_{2.5} during Atlanta rush hour:
695 Measurements of in-vehicle dithiothreitol (DTT) activity, *Atmos. Environ.*,

696 165, 169-178, 10.1016/j.atmosenv.2017.06.044, 2017.

697 Wang, J., Lin, X., Lu, L., Wu, Y., Zhang, H., Lv, Q., Liu, W., Zhang, Y., and Zhuang,
698 S.: Temporal variation of oxidative potential of water soluble components of
699 ambient PM_{2.5} measured by dithiothreitol (DTT) assay, *Sci. Total Environ.*,
700 649, 969-978, 10.1016/j.scitotenv.2018.08.375, 2019.

701 Wang, T., Huang, R. J., Li, Y., Chen, Q., Chen, Y., Yang, L., Guo, J., Ni, H., Hoffmann,
702 T., Wang, X., and Mai, B.: One-year characterization of organic aerosol
703 markers in urban Beijing: Seasonal variation and spatiotemporal comparison,
704 *Sci. Total Environ.*, 743, 140689, 10.1016/j.scitotenv.2020.140689, 2020a.

705 Wang, Y., Wang, M., Li, S., Sun, H., Mu, Z., Zhang, L., Li, Y., and Chen, Q.: Study on
706 the oxidation potential of the water-soluble components of ambient PM_{2.5} over
707 Xi'an, China: Pollution levels, source apportionment and transport pathways,
708 *Environ. Int.*, 136, 105515, 10.1016/j.envint.2020.105515, 2020b.

709 Wong, J. P. S., Tsagkaraki, M., Tsiodra, I., Mihalopoulos, N., Violaki, K., Kanakidou,
710 M., Sciare, J., Nenes, A., and Weber, R. J.: Effects of Atmospheric Processing
711 on the Oxidative Potential of Biomass Burning Organic Aerosols, *Environ. Sci.*
712 *Technol.*, 53, 6747-6756, 10.1021/acs.est.9b01034, 2019.

713 Wu, N., Lu, B., Chen, Q., Chen, J., and Li, X.: Connecting the Oxidative Potential of
714 Fractionated Particulate Matter With Chromophoric Substances, *J. Geophys.*
715 *Res-Atmos.*, 127, 10.1029/2021jd035503, 2022a.

716 Wu, N., Lyu, Y., Lu, B., Cai, D., Meng, X., and Li, X.: Oxidative potential induced by
717 metal-organic interaction from PM_{2.5} in simulated biological fluids, *Sci. Total*
718 *Environ.*, 848, 157768, 10.1016/j.scitotenv.2022.157768, 2022b.

719 Xing, C., Wang, Y., Yang, X., Zeng, Y., Zhai, J., Cai, B., Zhang, A., Fu, T. M., Zhu, L.,
720 Li, Y., Wang, X., and Zhang, Y.: Seasonal variation of driving factors of
721 ambient PM_{2.5} oxidative potential in Shenzhen, China, *Sci. Total Environ.*, 862,
722 160771, 10.1016/j.scitotenv.2022.160771, 2023.

723 Xiong, Q., Yu, H., Wang, R., Wei, J., and Verma, V.: Rethinking Dithiothreitol-Based
724 Particulate Matter Oxidative Potential: Measuring Dithiothreitol Consumption

725 versus Reactive Oxygen Species Generation, *Environ. Sci. Technol.*, 51, 6507-
726 6514, 10.1021/acs.est.7b01272, 2017.

727 Yalamanchili, J., Hennigan, C. J., and Reed, B. E.: Measurement artifacts in the
728 dithiothreitol (DTT) oxidative potential assay caused by interactions between
729 aqueous metals and phosphate buffer, *J. Hazard. Mater.*, 456, 131693, 2023.

730 Yu, H., Wei, J., Cheng, Y., Subedi, K., and Verma, V.: Synergistic and Antagonistic
731 Interactions among the Particulate Matter Components in Generating Reactive
732 Oxygen Species Based on the Dithiothreitol Assay, *Environ. Sci. Technol.*, 52,
733 2261–2270, 2018.

734 Yu, Q., Chen, J., Qin, W., Ahmad, M., Zhang, Y., Sun, Y., Xin, K., and Ai, J.:
735 Oxidative potential associated with water-soluble components of PM_{2.5} in
736 Beijing: The important role of anthropogenic organic aerosols, *J. Hazard.*
737 *Mater.*, 433, 128839, 10.1016/j.jhazmat.2022.128839, 2022a.

738 Yu, S., Liu, W., Xu, Y., Yi, K., Zhou, M., Tao, S., and Liu, W.: Characteristics and
739 oxidative potential of atmospheric PM_{2.5} in Beijing: Source apportionment and
740 seasonal variation, *Sci. Total Environ.*, 650, 277-287,
741 10.1016/j.scitotenv.2018.09.021, 2019.

742 Yu, Y., Sun, Q., Li, T., Ren, X., Lin, L., Sun, M., Duan, J., and Sun, Z.: Adverse
743 outcome pathway of fine particulate matter leading to increased cardiovascular
744 morbidity and mortality: An integrated perspective from toxicology and
745 epidemiology, *J. Hazard. Mater.*, 430, 128368, 10.1016/j.jhazmat.2022.128368,
746 2022b.

747 Yu, Y., Cheng, P., Li, Y., Gu, J., Gong, Y., Han, B., Yang, W., Sun, J., Wu, C., Song,
748 W., and Li, M.: The association of chemical composition particularly the
749 heavy metals with the oxidative potential of ambient PM_{2.5} in a megacity
750 (Guangzhou) of southern China, *Environ. Res.*, 213, 113489,
751 10.1016/j.envres.2022.113489, 2022c.

752 Yuan, W., Huang, R.-J., Luo, C., Yang, L., Cao, W., Guo, J., and Yang, H.:
753 Measurement report: Oxidation potential of water-soluble aerosol components

754 in the southern and northern of Beijing, Zenodo [data set],
755 <https://doi.org/10.5281/zenodo.10791126>, 2024.

756 Yuan, W., Huang, R.-J., Yang, L., Guo, J., Chen, Z., Duan, J., Wang, T., Ni, H., Han,
757 Y., Li, Y., Chen, Q., Chen, Y., Hoffmann, T., and O'Dowd, C.: Characterization
758 of the light-absorbing properties, chromophore composition and sources of
759 brown carbon aerosol in Xi'an, northwestern China, *Atmos. Chem. Phys.*, 20,
760 5129-5144, 10.5194/acp-20-5129-2020, 2020.

761 Zhang, Q., Ma, H., Li, J., Jiang, H., Chen, W., Wan, C., Jiang, B., Dong, G., Zeng, X.,
762 Chen, D., Lu, S., You, J., Yu, Z., Wang, X., and Zhang, G.: Nitroaromatic
763 Compounds from Secondary Nitrate Formation and Biomass Burning Are
764 Major Proinflammatory Components in Organic Aerosols in Guangzhou: A
765 Bioassay Combining High-Resolution Mass Spectrometry Analysis, *Environ.*
766 *Sci. Technol.*, 57, 21570-21580, <https://doi.org/10.1021/acs.est.3c04983>, 2023.

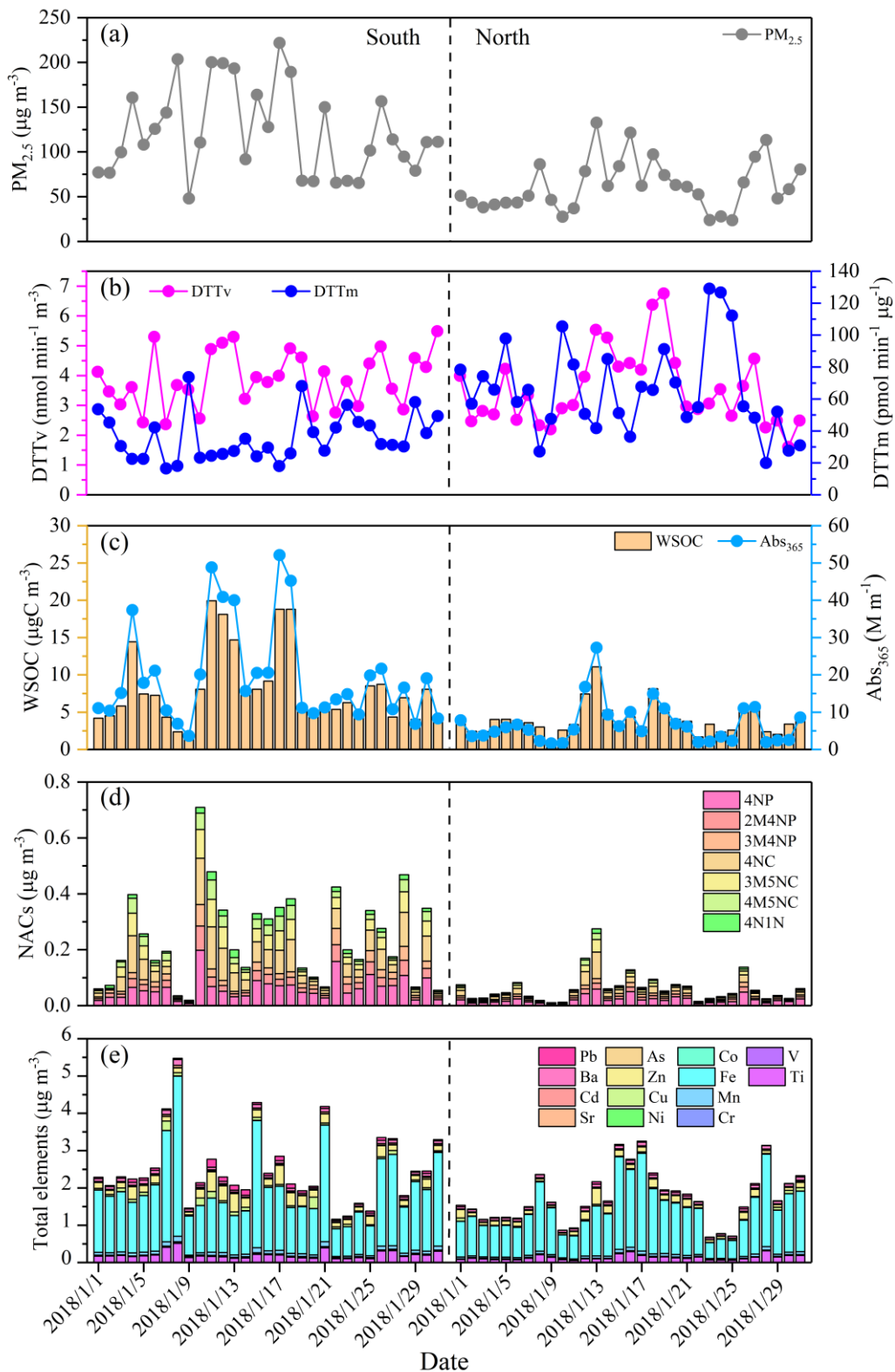
767 Zheng, Y., Davis, S. J., Persad, G. G., and Caldeira, K.: Climate effects of aerosols
768 reduce economic inequality, *Nat. Clim. Chang.*, 10, 220-224, 2020.

769

770

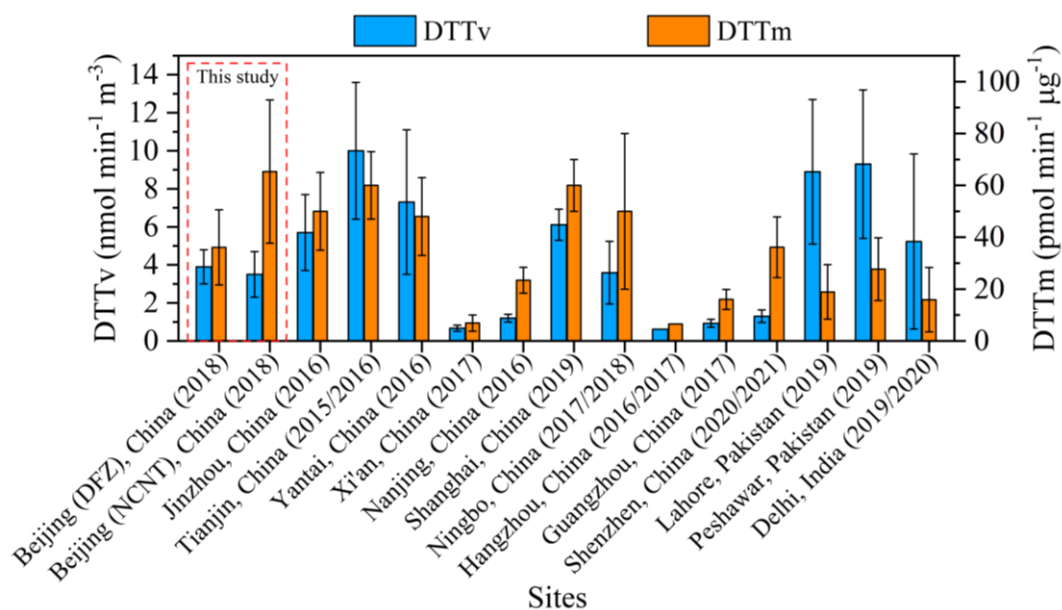
771

772



773

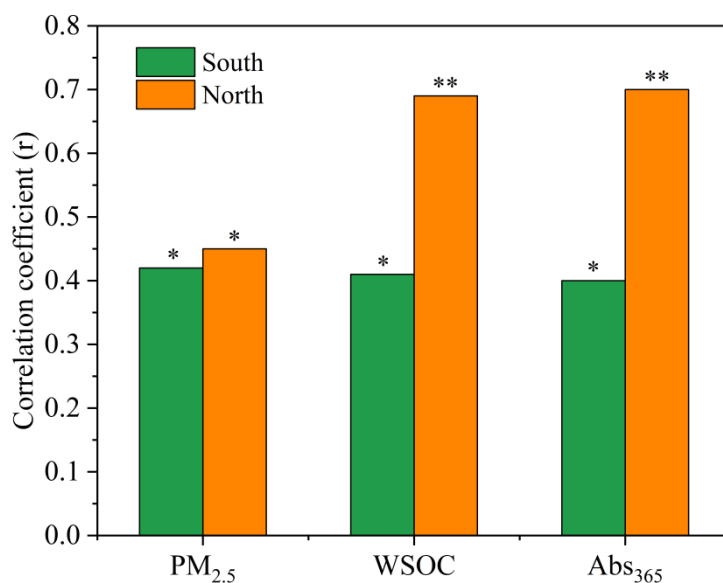
774 **Figure 1.** Time series of (a) PM_{2.5} concentration, (b) DTT_v and DTT_m, (c)
 775 concentration and light absorption at wavelength 365 nm (Abs₃₆₅) of WSOC,
 776 concentrations of (d) NACs and (e) elements.



777

778 **Figure 2.** Comparison of DTT_v and DTT_m values of water-soluble PM_{2.5} measured in
 779 this study with those measured in other areas of Asia during similar period.

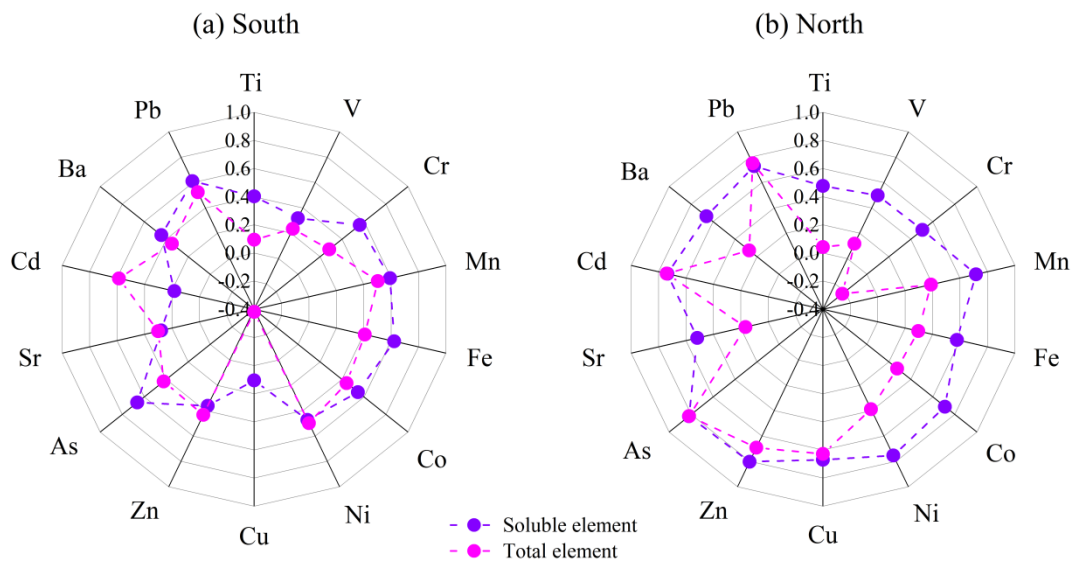
780



781

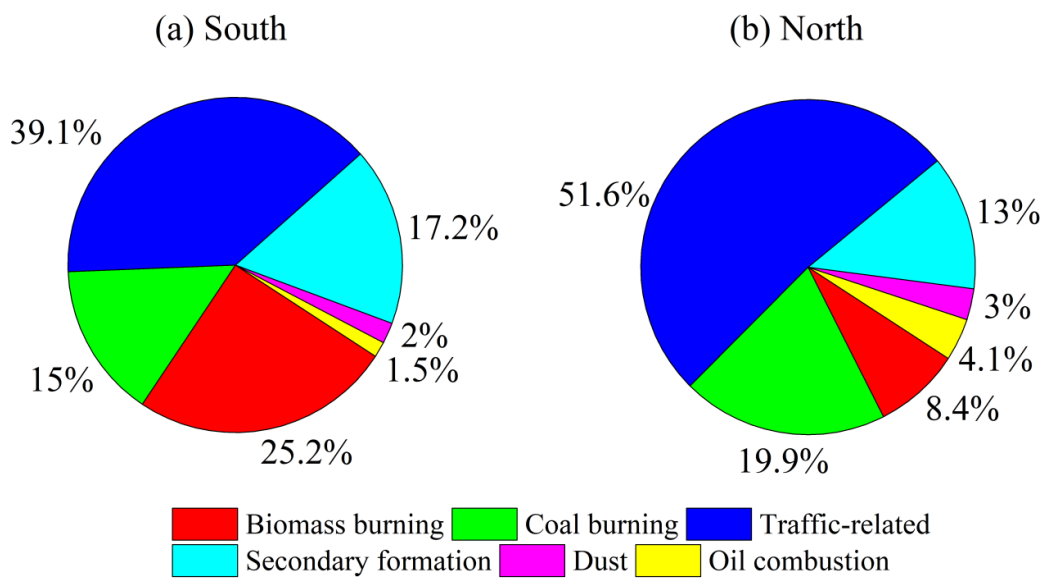
782 **Figure 3.** Correlation coefficients between DTT_v and PM_{2.5}, WSOC, and Abs₃₆₅ in the
 783 south and north of Beijing (* indicates correlation is significant at the 0.05 level, and
 784 ** indicates correlation is significant at the 0.01 level).

785



786
787
788
789

Figure 4. Correlation coefficients between DTT_v and elements in the (a) south and (b) north of Beijing.



790
791
792

Figure 5. Contributions of resolved sources to DTT_v in the (a) south and (b) north of Beijing.